Application of discontinuous Galerkin methods to shells and fracture of thin structures

G. Becker & Ludovic Noels

Computational & Multiscale Mechanics of Materials, ULg
Chemin des Chevreuils 1, B4000 Liège, Belgium
L.Noels@ulg.ac.be

R. Radovitzky, A. Seagraves, A. Jérusalem

EPFL – January 2010

Discontinuous Galerkin Methods

- Main idea
  - Finite-element discretization
  - Same **discontinuous** polynomial approximations for the
    - **Test** functions φ_h and
    - **Trial** functions $\delta\varphi$

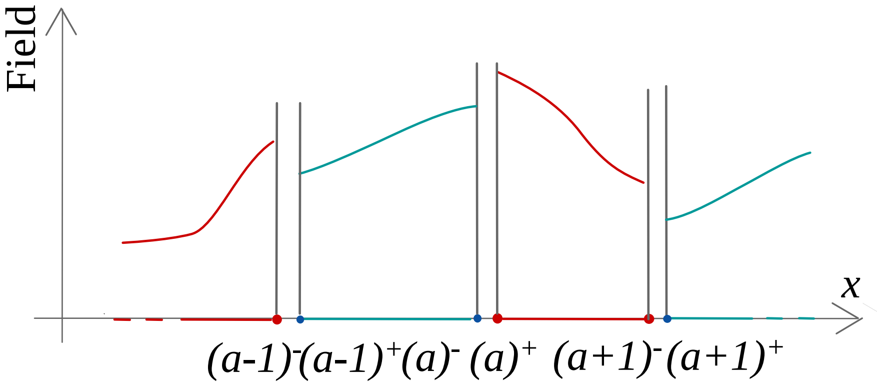

  - Definition of operators on the interface trace:
    - **Jump** operator: $[\![\bullet]\!] = \bullet^+ - \bullet^-$
    - **Mean** operator: $\langle\bullet\rangle = \frac{\bullet^+ + \bullet^-}{2}$
  - Continuity is weakly enforced, such that the method
    - Is consistent
    - Is stable
    - Has the optimal convergence rate

Discontinuous Galerkin Methods

- Discontinuous Galerkin methods vs Continuous
  - More expensive (more degrees of freedom)
  - More difficult to implement
  - …
- So why discontinuous Galerkin methods?
  - Weak enforcement of C^1 continuity for high-order equations
    - Shells with complex material behaviors
  - Exploitation of the discontinuous mesh to simulate dynamic fracture [Seagraves, Jérusalem, Noels, Radovitzky]:
    - Correct wave propagation before fracture
    - Easy to parallelize & scalable

Discontinuous Galerkin Methods

- Continuous field / discontinuous derivative
  - No new nodes
  - Weak enforcement of C^1 continuity
  - Displacement formulations of high-order differential equations
  - Usual shape functions in 3D (no new requirement)
  - Applications to
    - Beams, plates [Engel et al., CMAME 2002; Hansbo & Larson, CALCOLO 2002; Wells & Dung, CMAME 2007]
    - Linear & non-linear shells [Noels & Radovitzky, CMAME 2008; Noels IJNME 2009]
    - Damage & Strain Gradient [Wells et al., CMAME 2004; Molari, CMAME 2006; Bala-Chandran et al. 2008]

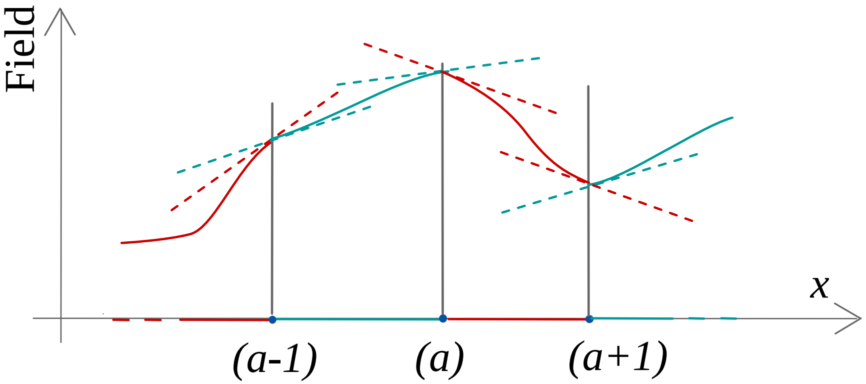

Université de Liège

Topics

- Key principles of DG methods
  - Illustration on volume FE
- Discontinuous Mesh & Dynamic Fracture
  - DG/Extrinsic cohesive law combination
- Kirchhoff-Love shells
  - C0/DG formulation of non-linear shells
- Dynamic Fracture of thin structures
  - Full DG formulation of beams
  - DG/Extrinsic cohesive law combination
- Conclusions & Perspectives

Key principles of DG methods

- Application to non-linear mechanics
  - Formulation in terms of the first Piola stress tensor $\mathbf{P}$

$$\boldsymbol{\nabla}_0 \cdot \mathbf{P}^T = 0 \text{ in } \Omega \quad \& \quad \begin{cases} \mathbf{P} \cdot \boldsymbol{N} = \bar{\boldsymbol{T}} \text{ on } \partial_N \Omega \\ \boldsymbol{\varphi}_h = \bar{\boldsymbol{\varphi}}_h \text{ on } \partial_D B \end{cases}$$

  - New weak formulation obtained by integration by parts **on each element** Ω^e

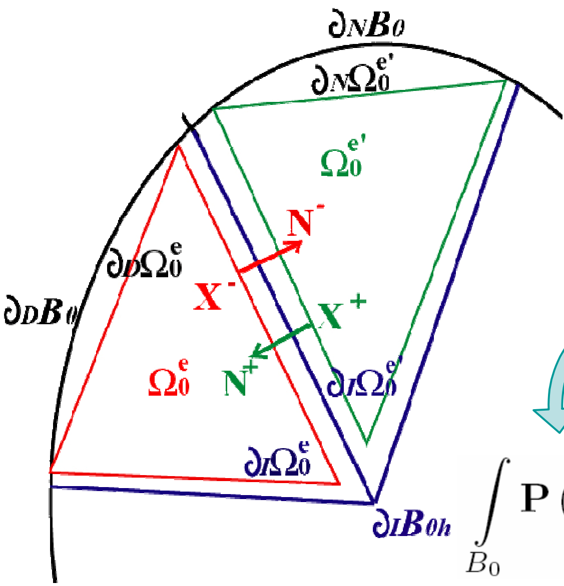

$$\sum_e \int_{\Omega_0^e} \boldsymbol{\nabla}_0 \cdot \mathbf{P}^T (\boldsymbol{\varphi}_h) \cdot \delta\boldsymbol{\varphi} \, dB = 0$$

$$\sum_e \int_{\Omega_0^e} -\mathbf{P}(\boldsymbol{\varphi}_h) : \boldsymbol{\nabla}_0 \delta\boldsymbol{\varphi} \, dB + \sum_e \int_{\partial\Omega_0^e} \delta\boldsymbol{\varphi} \cdot \mathbf{P}(\boldsymbol{\varphi}_h) \cdot \boldsymbol{N} \, d\partial B = 0$$

$$\int_{B_0} \mathbf{P}(\boldsymbol{\varphi}_h) : \boldsymbol{\nabla}_0 \delta\boldsymbol{\varphi} \, dB + \int_{\partial_I B_0} [\![\delta\boldsymbol{\varphi} \cdot \mathbf{P}(\boldsymbol{\varphi}_h)]\!] \cdot \boldsymbol{N}^- \, d\partial B = \int_{\partial_N B_0} \bar{\boldsymbol{T}} \cdot \delta\boldsymbol{\varphi} \, d\partial B$$

Key principles of DG methods

- Interface term rewritten as the sum of 3 terms
  - Introduction of the numerical flux ***h***

$$\int_{\partial_I B_0} [\![\delta\boldsymbol{\varphi}\cdot\mathbf{P}(\boldsymbol{\varphi}_h)]\!]\cdot\boldsymbol{N}^-\,d\partial B \rightarrow \int_{\partial_I B_0} [\![\delta\boldsymbol{\varphi}]\!]\cdot\boldsymbol{h}\left(\mathbf{P}^+,\,\mathbf{P}^-,\,\boldsymbol{N}^-\right)\,d\partial B$$

    - Has to be consistent: $\begin{cases}\boldsymbol{h}\left(\mathbf{P}^+,\,\mathbf{P}^-,\,\boldsymbol{N}^-\right) = -\boldsymbol{h}\left(\mathbf{P}^-,\,\mathbf{P}^+,\,\boldsymbol{N}^+\right)\\ \boldsymbol{h}\left(\mathbf{P}_{\text{exact}},\,\mathbf{P}_{\text{exact}},\,\boldsymbol{N}^-\right) = \mathbf{P}_{\text{exact}}\cdot\boldsymbol{N}^-\end{cases}$
    - One possible choice: $\boldsymbol{h}\left(\mathbf{P}^+,\,\mathbf{P}^-,\,\boldsymbol{N}^-\right) = \langle\mathbf{P}\rangle\cdot\boldsymbol{N}^-$
  - Weak enforcement of the compatibility

$$\int_{\partial_I B_0} [\![\boldsymbol{\varphi}_h]\!]\cdot\left\langle\frac{\partial\mathbf{P}}{\partial\mathbf{F}}:\boldsymbol{\nabla}_0\delta\boldsymbol{\varphi}\right\rangle\cdot\boldsymbol{N}^-\,d\partial B$$

  - Stabilization controlled by parameter β, for all mesh sizes h^s

$$\int_{\partial_I B_0} [\![\boldsymbol{\varphi}_h]\!]\otimes\boldsymbol{N}^-:\left\langle\frac{\beta}{h^s}\frac{\partial\mathbf{P}}{\partial\mathbf{F}}\right\rangle:[\![\delta\boldsymbol{\varphi}]\!]\otimes\boldsymbol{N}^-\,d\partial B$$

Noels & Radovitzky, IJNME 2006 & JAM 2006

  - Those terms can also be explicitly derived from a variational formulation (Hu-Washizu-de Veubeke functional)

Key principles of DG methods

- Numerical applications
  - Properties for a polynomial approximation of order k
    - Consistent, stable for $\beta > C^k$, convergence in the e-norm in k
    - Explicit time integration with conditional stability $\Delta t_{\text{crit}} = \frac{h^s}{\sqrt{\beta}}\sqrt{\frac{\rho_0}{E}}$
    - High scalability
  - Examples

Taylor's impact

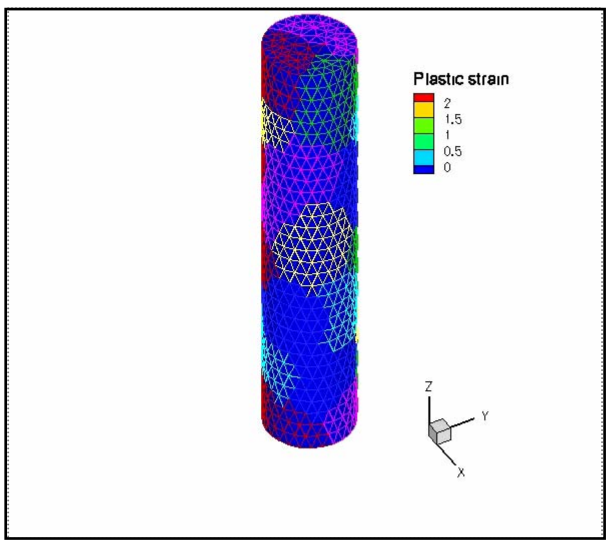

Wave propagation

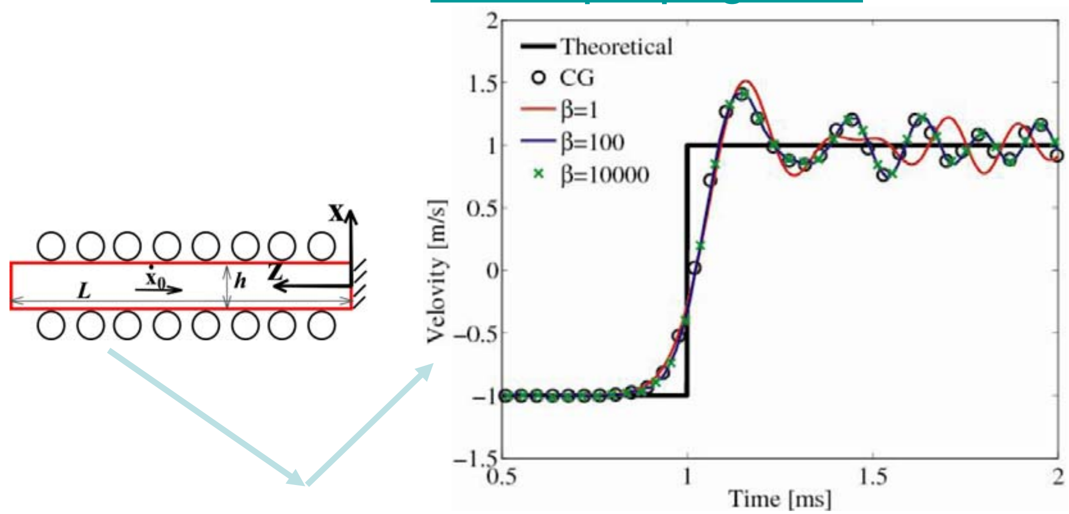

Time evolution of the free face velocity

Discontinuous Mesh & Dynamic Fracture

- Dynamic fracture
  - Fracture: a gradual process of separation which occurs in small regions of material adjacent to the tip of a forming crack: the cohesive zone [Dugdale 1960, Barrenblatt 1962, …]
  - Separation is resisted to by a cohesive traction
  - 2-parameter cohesive law
    - Peak cohesive traction σ_{max} (spall strength)
    - Fracture energy G_c
    - Automatically accounts for time scale [Camacho & Ortiz, 1996]
    - Intrinsic law vs Extrinsic law

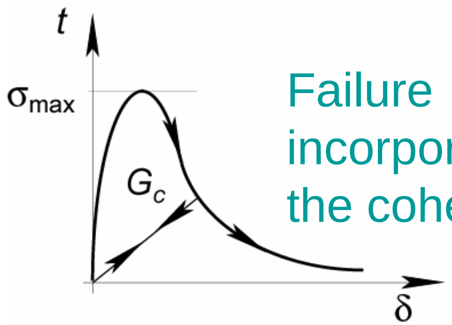

Failure criterion incorporated within the cohesive law

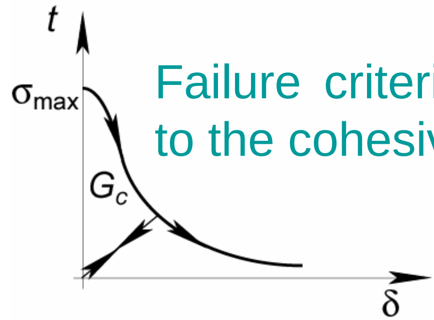

Failure criterion external to the cohesive law

Discontinuous Mesh & Dynamic Fracture

- Finite element discretization & interface elements
  - The cohesive law is integrated on an interface element inserted between two adjacent tetrahedra [Ortiz & Pandolfi 1999]
  - Potential structure of the cohesive law: [Ortiz & Pandolfi 1999]
    - Effective opening in terms of β_c the ratio between the shear and normal critical tractions:

$$\delta = \sqrt{\underbrace{\left|[\![\varphi]\!] \cdot \boldsymbol{N}^-\right|^2}_{\delta_n^2 = \|\boldsymbol{\delta}_n\|^2} + \beta_c^2 \underbrace{\left\|[\![\varphi]\!] - [\![\varphi]\!] \cdot \boldsymbol{N}^- \boldsymbol{N}^-\right\|^2}_{\delta_s^2 = \|\boldsymbol{\delta}_s\|^2}}$$

    - Definition of a potential: $\phi = \phi(\delta)$
    - Interface traction: $\boldsymbol{t} = \dfrac{\partial \phi}{\partial \boldsymbol{\delta}} = \dfrac{\partial \phi}{\partial \delta_n} \boldsymbol{N}^- + \dfrac{\partial \phi}{\partial \delta_s} \dfrac{\boldsymbol{\delta_s}}{\delta_s}$

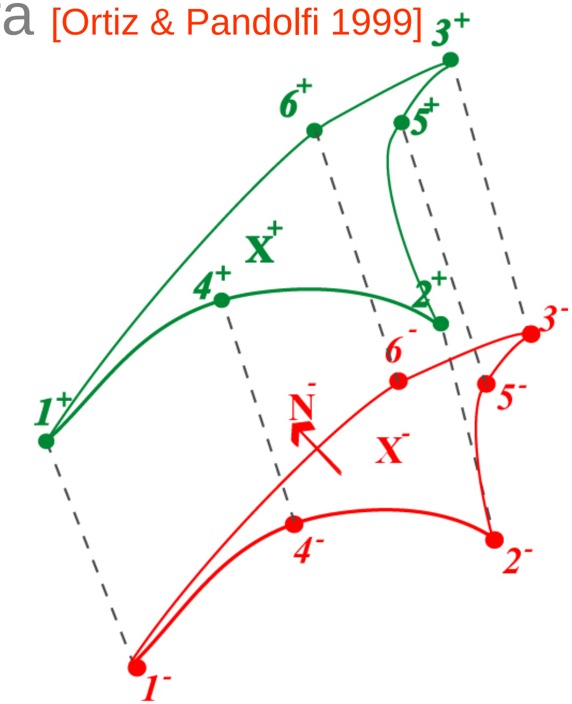

Discontinuous Mesh & Dynamic Fracture

- Two methods
  - Intrinsic Law
    - Cohesive elements inserted from the beginning
    - Drawbacks:
      - Efficient if a priori knowledge of the crack path
      - Mesh dependency [Xu & Needelman, 1994]
      - Initial slope modifies the effective elastic modulus
      - This slope should tend to infinity [Klein et al. 2001]:
        - » Alteration of a wave propagation
        - » Critical time step is reduced

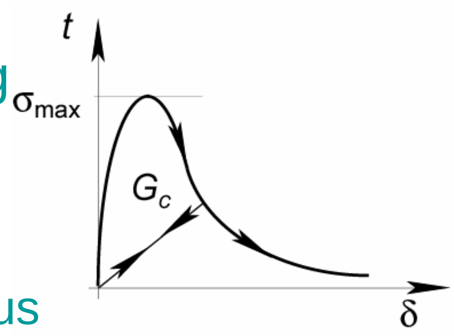

  - Extrinsic Law
    - Cohesive elements inserted on the fly when failure criterion is verified [Ortiz & Pandolfi 1999]
    - Drawback
      - Complex implementation in 3D (parallelization)

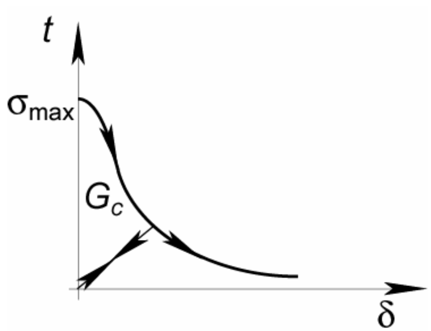

- New DG/extrinsic method [Seagraves, Jerusalem, Radovitzky, Noels]
  - Interface elements inserted from the beginning
  - Interface law corresponds initially to the DG interface forces

Discontinuous Mesh & Dynamic Fracture

- New DG/extrinsic method:

  [Seagraves, Jerusalem, Radovitzky, Noels]

  – Numerical application: the spall test

    - Two opposite waves interact at the center of the specimen
    - The interaction leads to stresses higher than the spall stress
    - The specimen breaks exactly at its middle

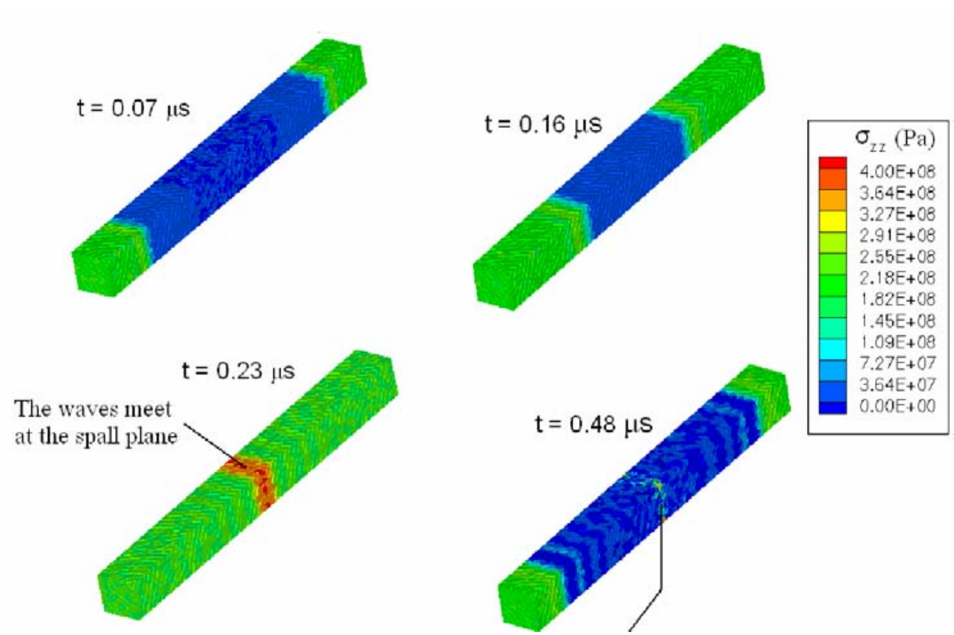

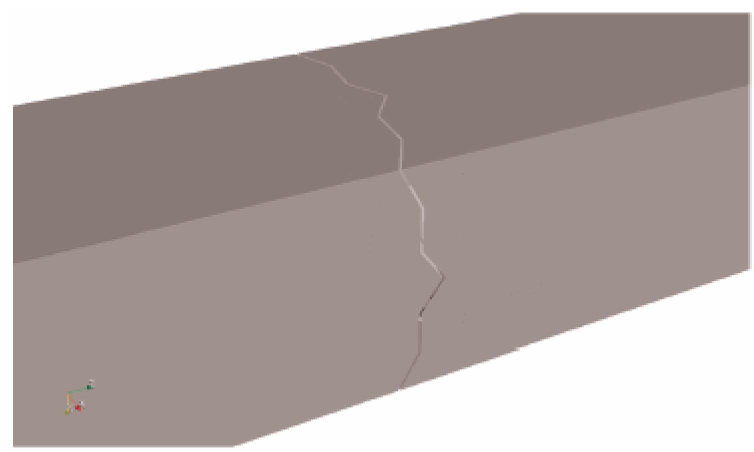

Discontinuous Galerkin Methods

- Continuous field / discontinuous derivative
  - No new nodes
  - Weak enforcement of C^1 continuity
  - Displacement formulations of high-order differential equations
  - Usual shape functions in 3D (no new requirement)
  - Applications to
    - Beams, plates [Engel et al., CMAME 2002; Hansbo & Larson, CALCOLO 2002; Wells & Dung, CMAME 2007]
    - Linear & non-linear shells [Noels & Radovitzky, CMAME 2008; Noels IJNME 2009]
    - Damage & Strain Gradient [Wells et al., CMAME 2004; Molari, CMAME 2006; Bala-Chandran et al. 2008]

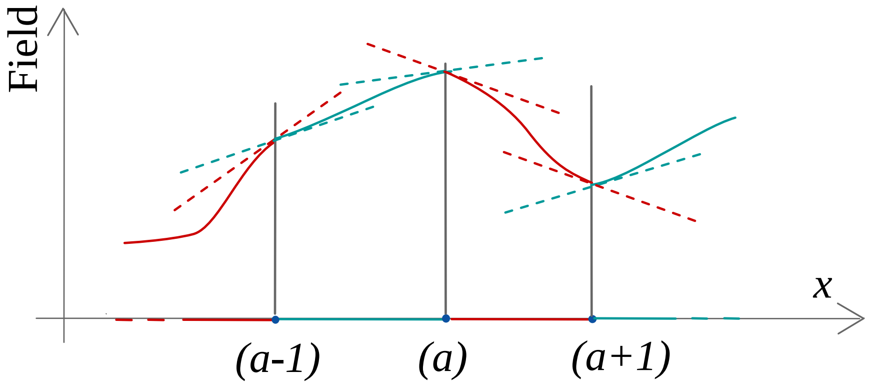

Kirchhoff-Love Shells

- Description of the thin body

$$\boldsymbol{x} = \boldsymbol{\Phi}\left(\xi^I\right) = \boldsymbol{\varphi}\left(\xi^\alpha\right) + \xi^3 \lambda_h \boldsymbol{t}\left(\xi^\alpha\right)$$

Mapping of the mid-surface

Thickness stretch

Mapping of the normal to the mid-surface

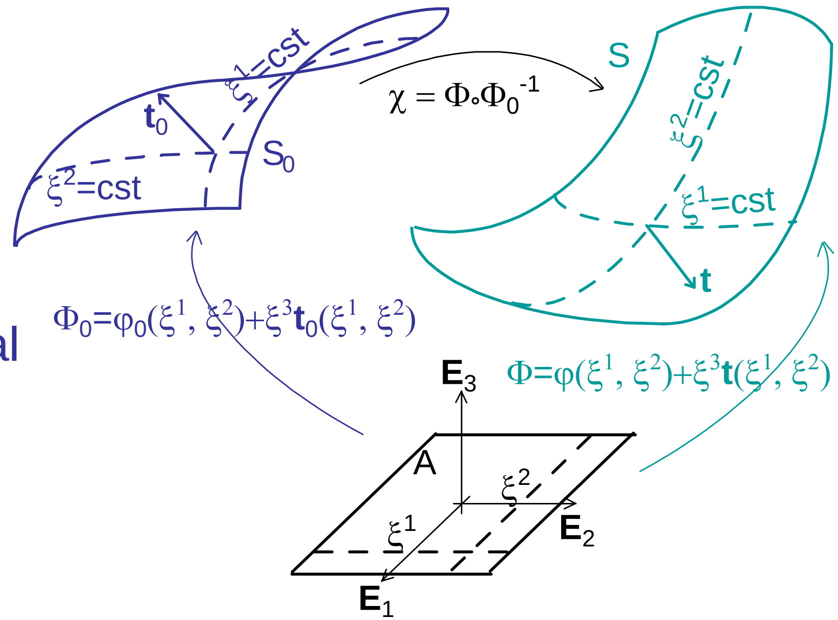

- Deformation mapping

$\mathbf{F} = \boldsymbol{\nabla}\boldsymbol{\Phi} \circ \left[\boldsymbol{\nabla}\boldsymbol{\Phi}_0\right]^{-1}$ with

$\boldsymbol{\nabla}\boldsymbol{\Phi} = \boldsymbol{g}_i \otimes \boldsymbol{E}^i$ & $\boldsymbol{g}_i = \boldsymbol{\nabla}\boldsymbol{\Phi}\boldsymbol{E}_i = \dfrac{\partial \boldsymbol{\Phi}}{\partial \xi^i}$

$\Longrightarrow$ $\boldsymbol{g}_\alpha = \dfrac{\partial \boldsymbol{\Phi}}{\partial \xi^\alpha} = \boldsymbol{\varphi}_{,\alpha} + \xi^3 \lambda_h \boldsymbol{t}_{,\alpha} + \xi^3 \boldsymbol{t} \lambda_{h,\alpha}$ & $\boldsymbol{g}_3 = \dfrac{\partial \boldsymbol{\Phi}}{\partial \xi^3} = \lambda_h \boldsymbol{t}$

- Shearing is neglected

$\Longrightarrow$ $\boldsymbol{t} = \dfrac{\boldsymbol{\varphi}_{,1} \wedge \boldsymbol{\varphi}_{,2}}{\left\|\boldsymbol{\varphi}_{,1} \wedge \boldsymbol{\varphi}_{,2}\right\|}$ & the gradient of thickness stretch $\lambda_{h,\alpha}$ neglected

Higher order equation

Kirchhoff-Love Shells

- Resultant equilibrium equations:
  - Linear momentum $\frac{1}{\bar{j}}\left(\bar{j}\boldsymbol{n}^{\alpha}\right)_{,\alpha} + \boldsymbol{n}^{\mathcal{A}} = 0$
  - Angular momentum $\frac{1}{\bar{j}}\left(\bar{j}\tilde{\boldsymbol{m}}^{\alpha}\right)_{,\alpha} - \boldsymbol{l} + \lambda\boldsymbol{t} + \tilde{\boldsymbol{m}}^{\mathcal{A}} = 0$
  - In terms of resultant stresses:

$$\begin{cases} \boldsymbol{n}^{\alpha} = \frac{1}{\bar{j}}\int_{h_{\min 0}}^{h_{\max 0}} \boldsymbol{\sigma}\boldsymbol{g}^{\alpha}\det\left(\boldsymbol{\nabla\Phi}\right) d\xi^{3} \\ \tilde{\boldsymbol{m}}^{\alpha} = \frac{1}{\bar{j}}\int_{h_{\min 0}}^{h_{\max 0}} \xi^{3}\boldsymbol{\sigma}\boldsymbol{g}^{\alpha}\det\left(\boldsymbol{\nabla\Phi}\right) d\xi^{3} \\ \boldsymbol{l} = \frac{1}{\bar{j}}\int_{h_{\min 0}}^{h_{\max 0}} \boldsymbol{\sigma}\boldsymbol{g}^{3}\det\left(\boldsymbol{\nabla\Phi}\right) d\xi^{3} \end{cases}$$

    of resultant applied tension $\boldsymbol{n}^{\mathcal{A}}$ and torque $\tilde{\boldsymbol{m}}^{\mathcal{A}}$

    and of the mid-surface Jacobian $\bar{j} = \|\boldsymbol{\varphi}_{,1} \wedge \boldsymbol{\varphi}_{,2}\|$

Kirchhoff-Love Shells

- Non-linear material behavior
  - Through the thickness integration by Simpson's rule
  - At each Simpson point
    - Internal energy $W(\mathbf{C}=\mathbf{F}^T\mathbf{F})$ with

$$\begin{cases} \mathbf{C} = \boldsymbol{g}_i \cdot \boldsymbol{g}_j \; \boldsymbol{g}_0^i \otimes \boldsymbol{g}_0^j = \mathrm{g}_{ij} \; \boldsymbol{g}_0^i \otimes \boldsymbol{g}_0^j \\ \boldsymbol{\sigma} = \sigma^{ij} \; \boldsymbol{g}_i \otimes \boldsymbol{g}_j = 2 \frac{\det(\boldsymbol{\nabla \Phi}_0)}{\det(\boldsymbol{\nabla \Phi})} \frac{\partial W}{\partial \mathrm{g}_{ij}} \boldsymbol{g}_i \otimes \boldsymbol{g}_j \end{cases}$$

    - Iteration on the thickness ratio $\lambda_h = \frac{h_{\max} - h_{\min}}{h_{\max 0} - h_{\min 0}}$ in order to reach the plane stress assumption $\sigma^{33}=0$

  - Simpson's rule leads to the resultant stresses:

$$\begin{cases} \boldsymbol{n}^\alpha = \frac{1}{\bar{j}} \int_{h_{\min 0}}^{h_{\max 0}} \boldsymbol{\sigma} \boldsymbol{g}^\alpha \det(\boldsymbol{\nabla \Phi}) \, d\xi^3 \\ \tilde{\boldsymbol{m}}^\alpha = \frac{1}{\bar{j}} \int_{h_{\min 0}}^{h_{\max 0}} \xi^3 \boldsymbol{\sigma} \boldsymbol{g}^\alpha \det(\boldsymbol{\nabla \Phi}) \, d\xi^3 \\ \boldsymbol{l} = \frac{1}{\bar{j}} \int_{h_{\min 0}}^{h_{\max 0}} \boldsymbol{\sigma} \boldsymbol{g}^3 \det(\boldsymbol{\nabla \Phi}) \, d\xi^3 \end{cases}$$

Kirchhoff-Love Shells

- Non-linear discontinuous Galerkin formulation
  - New weak form obtained from the momentum equations
  - Integration by parts on each element $\mathcal{A}^e$
  - Across 2 elements $\delta \boldsymbol{t}$ is discontinuous

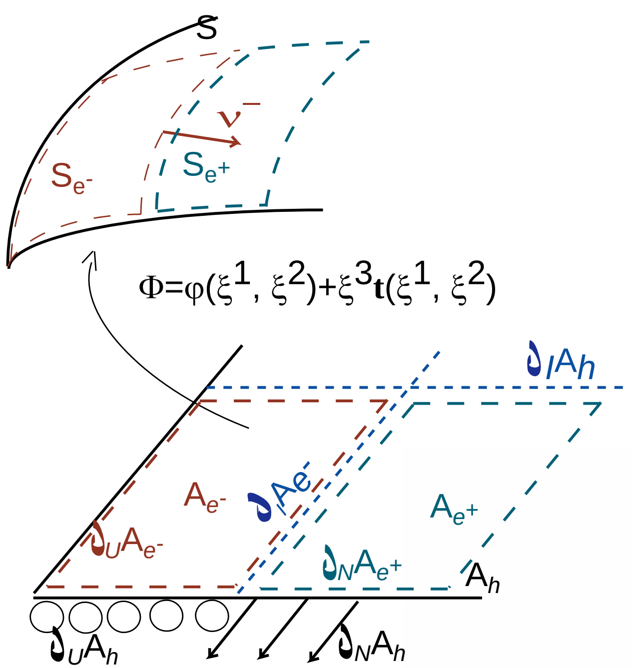

$$0 = \int_{\mathcal{A}_e} \left(\bar{j}\boldsymbol{n}^{\alpha}(\boldsymbol{\varphi}_h)\right)_{,\alpha} \cdot \delta\boldsymbol{\varphi} d\mathcal{A} + \int_{\mathcal{A}_e} \boldsymbol{n}^{\mathcal{A}} \cdot \delta\boldsymbol{\varphi}\bar{j} d\mathcal{A} + \int_{\mathcal{A}_e} \left[\left(\bar{j}\tilde{\boldsymbol{m}}^{\alpha}(\boldsymbol{\varphi}_h)\right)_{,\alpha} - \bar{j}\boldsymbol{l}\right] \cdot \delta\boldsymbol{t}\lambda_h d\mathcal{A} + \int_{\mathcal{A}_e} \tilde{\boldsymbol{m}}^{\mathcal{A}} \cdot \delta\boldsymbol{t}\lambda_h \bar{j} d\mathcal{A}$$

$$-\sum_e \int_{\bar{\mathcal{A}}_e} \bar{j}\tilde{\boldsymbol{m}}^{\alpha}(\boldsymbol{\varphi}_h) \cdot (\delta\boldsymbol{t}\lambda_h)_{,\alpha} d\mathcal{A} + \sum_e \int_{\partial\mathcal{A}_e} \bar{j}\tilde{\boldsymbol{m}}^{\alpha}(\boldsymbol{\varphi}_h) \cdot \delta\boldsymbol{t}\lambda_h \nu_\alpha d\mathcal{A}$$

$$\int_{\mathcal{A}_h} \bar{j}\boldsymbol{n}^{\alpha}(\boldsymbol{\varphi}_h) \cdot \delta\boldsymbol{\varphi}_{,\alpha} d\mathcal{A} + \int_{\mathcal{A}_h} \bar{j}\boldsymbol{l} \cdot \delta\boldsymbol{t}\lambda_h d\mathcal{A} + \int_{\mathcal{A}_h} \bar{j}\tilde{\boldsymbol{m}}^{\alpha}(\boldsymbol{\varphi}_h) \cdot (\delta\boldsymbol{t}\lambda_h)_{,\alpha} d\mathcal{A} + \int_{\partial_I\mathcal{A}_h \cup \partial_T\mathcal{A}_h} [\![\delta\boldsymbol{t} \cdot \bar{j}\lambda_h\tilde{\boldsymbol{m}}^{\alpha}]\!] \nu_\alpha^- d\partial\mathcal{A} = \int_{\partial_N\mathcal{A}_h} \bar{j}\bar{\boldsymbol{n}} \cdot \delta\boldsymbol{\varphi} d\mathcal{A} + \int_{\partial_M\mathcal{A}_h} \bar{j}\bar{\tilde{\boldsymbol{m}}} \cdot \delta\boldsymbol{t}\lambda_h d\mathcal{A} + \int_{\mathcal{A}_h} \boldsymbol{n}^{\mathcal{A}} \cdot \delta\boldsymbol{\varphi}\bar{j} d\mathcal{A} + \int_{\mathcal{A}_h} \tilde{\boldsymbol{m}}^{\mathcal{A}} \cdot \delta\boldsymbol{t}\lambda_h\bar{j} d\mathcal{A}$$

Kirchhoff-Love Shells

- Interface terms rewritten as the sum of 3 terms
  - Introduction of the numerical flux $\boldsymbol{h}$

$$\int_{\partial_I \mathcal{A}_h} [\![\bar{j}\tilde{\boldsymbol{m}}^{\alpha}(\boldsymbol{\varphi}_h)\cdot\delta\boldsymbol{t}\lambda_h]\!]\,\nu_{\alpha}^{-}\,d\mathcal{A} \rightarrow \int_{\partial_I \mathcal{A}_h} [\![\delta\boldsymbol{t}]\!]\cdot\boldsymbol{h}\left(\left(\bar{j}\lambda_h\tilde{\boldsymbol{m}}^{\alpha}\right)^{+},\,\left(\bar{j}\lambda_h\tilde{\boldsymbol{m}}^{\alpha}\right)^{-},\,\nu_{\alpha}^{-}\right)d\mathcal{A}$$

    - Has to be consistent: $\boldsymbol{h}\left(\lambda_h\bar{j}\tilde{\boldsymbol{m}}^{\alpha}_{\text{exact}},\,\bar{j}\lambda_h\tilde{\boldsymbol{m}}^{\alpha}_{\text{exact}},\,\nu_{\alpha}\right)=\lambda_h\bar{j}\tilde{\boldsymbol{m}}^{\alpha}_{\text{exact}}\nu_{\alpha}^{-}$
    - One possible choice: $\boldsymbol{h}\left(\left(\bar{j}\lambda_h\tilde{\boldsymbol{m}}^{\alpha}\right)^{+},\,\left(\bar{j}\lambda_h\tilde{\boldsymbol{m}}^{\alpha}\right)^{-},\,\nu_{\alpha}^{-}\right)=\nu_{\alpha}^{-}\left\langle\bar{j}\lambda_h\tilde{\boldsymbol{m}}^{\alpha}\right\rangle$
  - Weak enforcement of the compatibility

$$\int_{\partial_I \mathcal{A}_h} [\![\boldsymbol{t}(\boldsymbol{\varphi}_h)]\!]\cdot\left\langle\delta\left(\bar{j}\lambda_h\tilde{\boldsymbol{m}}^{\alpha}\right)\right\rangle\nu_{\alpha}^{-}\,d\partial\mathcal{A}$$

Linearization leads to the material tangent modulii $\mathcal{H}_m$

$$\int_{\partial_I \mathcal{A}_h} [\![\boldsymbol{t}(\boldsymbol{\varphi}_h)]\!]\cdot\left\langle\bar{j}_0\mathcal{H}_m^{\alpha\beta\gamma\delta}\left(\delta\boldsymbol{\varphi}_{,\gamma}\cdot\boldsymbol{t}_{,\delta}+\boldsymbol{\varphi}_{,\gamma}\cdot\delta\boldsymbol{t}_{,\delta}\right)\boldsymbol{\varphi}_{,\beta}+\bar{j}\lambda_h\tilde{\boldsymbol{m}}^{\alpha}\cdot\boldsymbol{\varphi}_{,\beta}\;\delta\boldsymbol{\varphi}_{,\beta}\right\rangle\nu_{\alpha}^{-}\,d\partial\mathcal{A}$$

  - Stabilization controlled by parameter β, for all mesh sizes h^s

$$\int_{\partial_I \mathcal{A}_h\cup\partial_T\mathcal{A}_h} [\![\boldsymbol{t}(\boldsymbol{\varphi}_h)]\!]\cdot\boldsymbol{\varphi}_{,\beta}\left\langle\frac{\beta\bar{j}_0\mathcal{H}_m^{\alpha\beta\gamma\delta}}{h^s}\right\rangle[\![\delta\boldsymbol{t}]\!]\cdot\boldsymbol{\varphi}_{,\gamma}\nu_{\alpha}^{-}\nu_{\delta}^{-}\,d\partial\mathcal{A}$$

Kirchhoff-Love Shells

- New weak formulation

$$\int_{\mathcal{A}_h} \bar{j}\boldsymbol{n}^{\alpha}(\boldsymbol{\varphi}_h)\cdot\delta\boldsymbol{\varphi}_{,\alpha}\,d\mathcal{A} + \int_{\mathcal{A}_h} \bar{j}\tilde{\boldsymbol{m}}^{\alpha}(\boldsymbol{\varphi}_h)\cdot(\delta\boldsymbol{t}\lambda_h)_{,\alpha}\,d\mathcal{A} + \int_{\mathcal{A}_h} \bar{j}\boldsymbol{l}\cdot\delta\boldsymbol{t}\lambda_h\,d\mathcal{A} +$$

$$\int_{\partial_I\mathcal{A}_h\cup\partial_T\mathcal{A}_h} [\![\boldsymbol{t}(\boldsymbol{\varphi}_h)]\!]\cdot\left\langle \bar{j}_0\mathcal{H}_m^{\alpha\beta\gamma\delta}\left(\delta\boldsymbol{\varphi}_{,\gamma}\cdot\boldsymbol{t}_{,\delta}+\boldsymbol{\varphi}_{,\gamma}\cdot\delta\boldsymbol{t}_{,\delta}\right)\boldsymbol{\varphi}_{,\beta} + \bar{j}\lambda_h\tilde{\boldsymbol{m}}^{\alpha}\cdot\boldsymbol{\varphi}_{,\beta}\;\;\delta\boldsymbol{\varphi}_{,\beta}\right\rangle \nu^-_{\alpha}\,d\partial\mathcal{A}$$

$$\int_{\partial_I\mathcal{A}_h\cup\partial_T\mathcal{A}_h} [\![\delta\boldsymbol{t}]\!]\cdot\left\langle \bar{j}\lambda_h\tilde{\boldsymbol{m}}^{\alpha}\right\rangle \nu^-_{\alpha}\,d\partial\mathcal{A} + \int_{\partial_I\mathcal{A}_h\cup\partial_T\mathcal{A}_h} [\![\boldsymbol{t}(\boldsymbol{\varphi}_h)]\!]\cdot\boldsymbol{\varphi}_{,\beta}\left\langle\frac{\beta\bar{j}_0\mathcal{H}_m^{\alpha\beta\gamma\delta}}{h^s}\right\rangle[\![\delta\boldsymbol{t}]\!]\cdot\boldsymbol{\varphi}_{,\gamma}\nu^-_{\alpha}\nu^-_{\delta}\,d\partial\mathcal{A} =$$

$$\int_{\partial_N\mathcal{A}_h} \bar{j}\bar{\boldsymbol{n}}\cdot\delta\boldsymbol{\varphi}\,d\mathcal{A} + \int_{\partial_M\mathcal{A}_h} \bar{j}\bar{\tilde{\boldsymbol{m}}}\cdot\delta\boldsymbol{t}\lambda_h\,d\mathcal{A} + \int_{\mathcal{A}_h} \boldsymbol{n}^{\mathcal{A}}\cdot\delta\boldsymbol{\varphi}\bar{j}\,d\mathcal{A} + \int_{\mathcal{A}_h} \tilde{\boldsymbol{m}}^{\mathcal{A}}\cdot\delta\boldsymbol{t}\lambda_h\bar{j}\,d\mathcal{A}$$

- Implementation
  - Shell elements
    - Membrane and bending responses
    - 2x2 (4x4) Gauss points for bi-quadratic (bi-cubic) quadrangles
  - Interface elements
    - 3 contributions
    - 2 (4) Gauss points for quadratic (cubic) meshes
    - Contributions of neighboring shells evaluated at these points

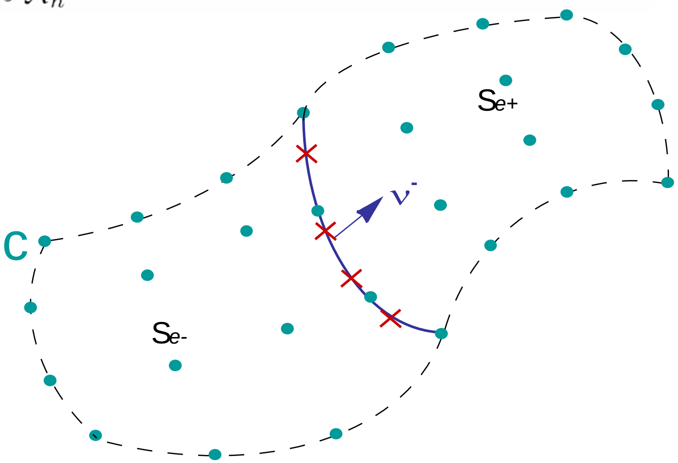

Kirchhoff-Love Shells

- Pinched open hemisphere
  - Properties:
    - 18-degree hole
    - Thickness 0.04 m; Radius 10 m
    - Young 68.25 MPa; Poisson 0.3
  - Comparison of the DG methods
    - Quadratic, cubic & distorted el.

    with literature

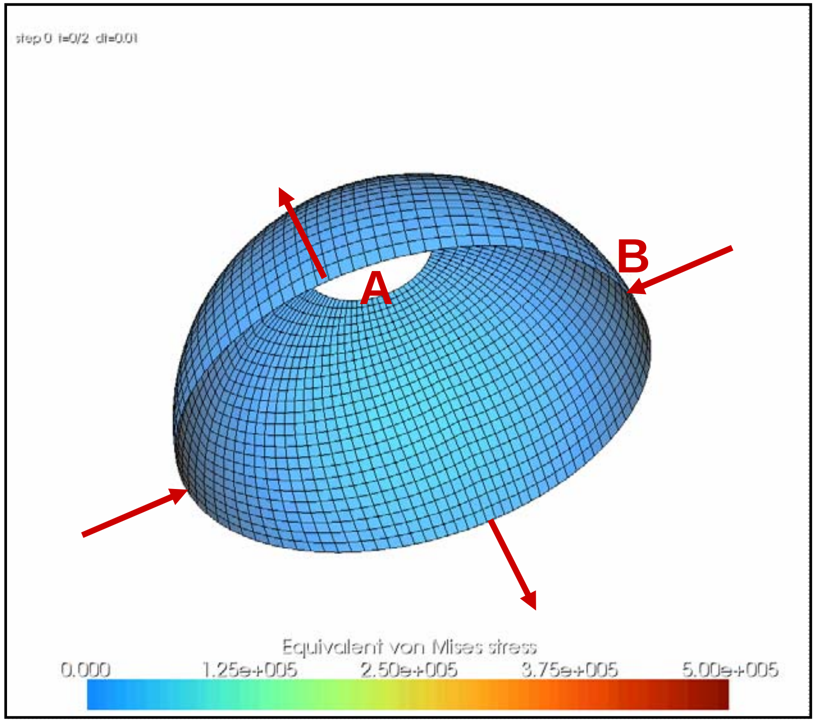

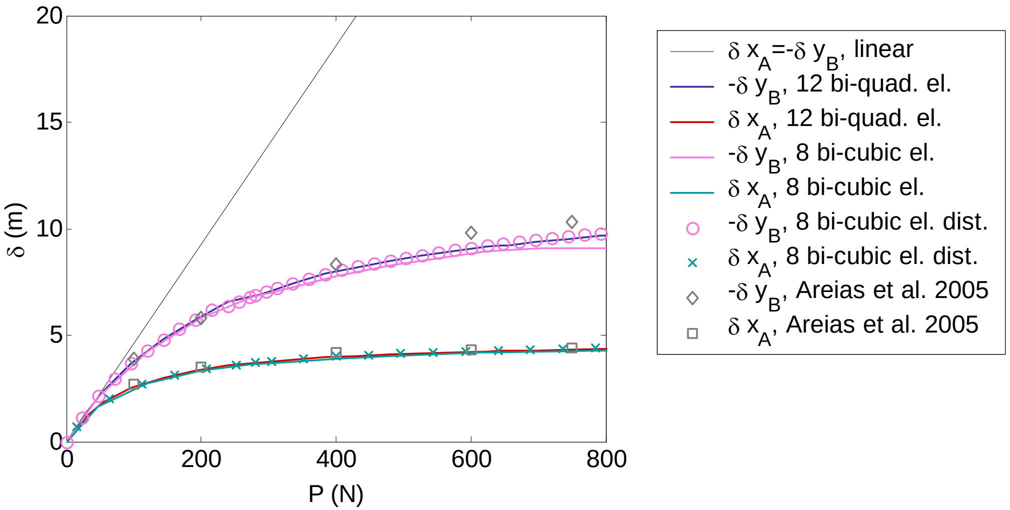

- Pinched open hemisphere

Influence of the stabilization parameter

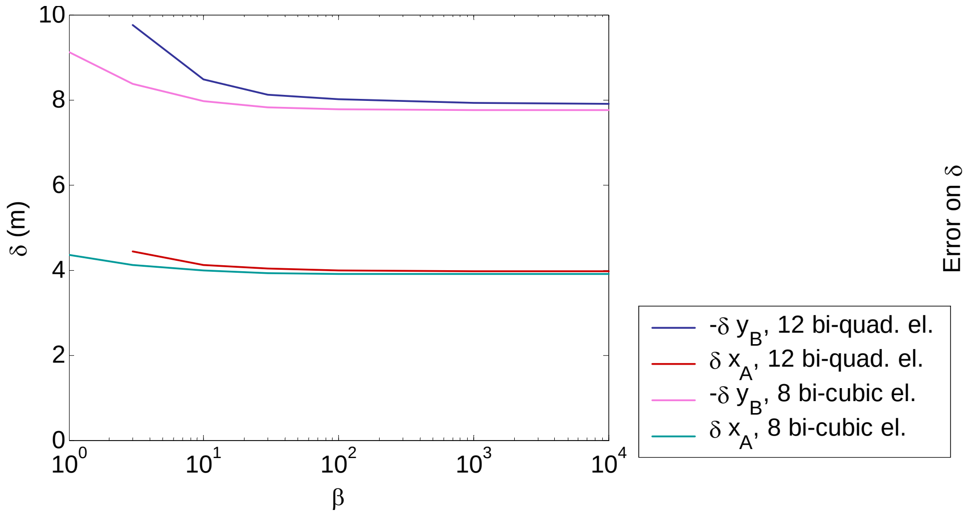

Influence of the mesh size

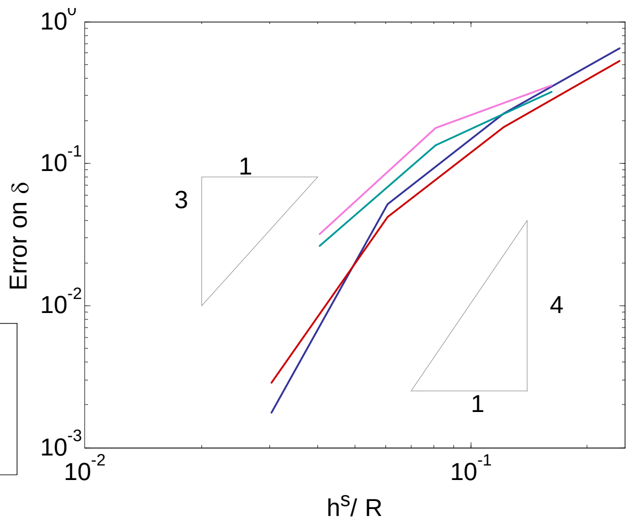

  - Stability if $\beta > 10$
  - Order of convergence in the L^2-norm in k+1

Kirchhoff-Love Shells

- Plate ring
  - Properties:
    - Radii 6 -10 m
    - Thickness 0.03 m
    - Young 12 GPa; Poisson 0
  - Comparison of DG methods
    - Quadratic elements

    with literature

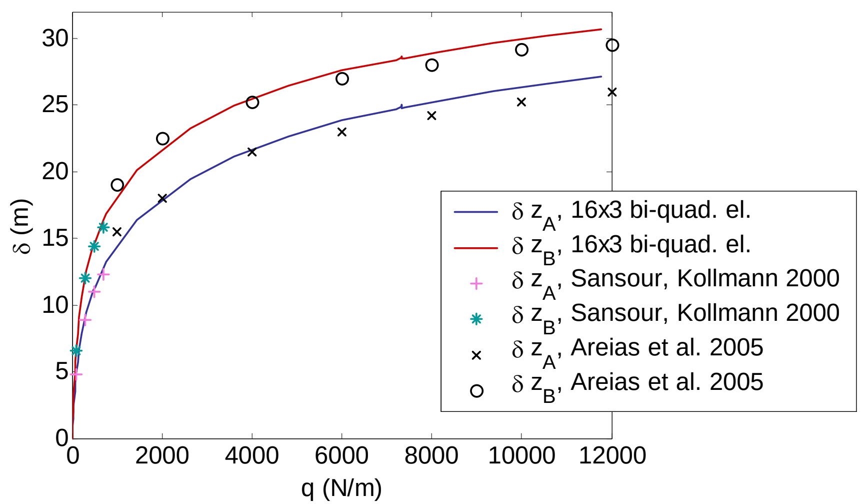

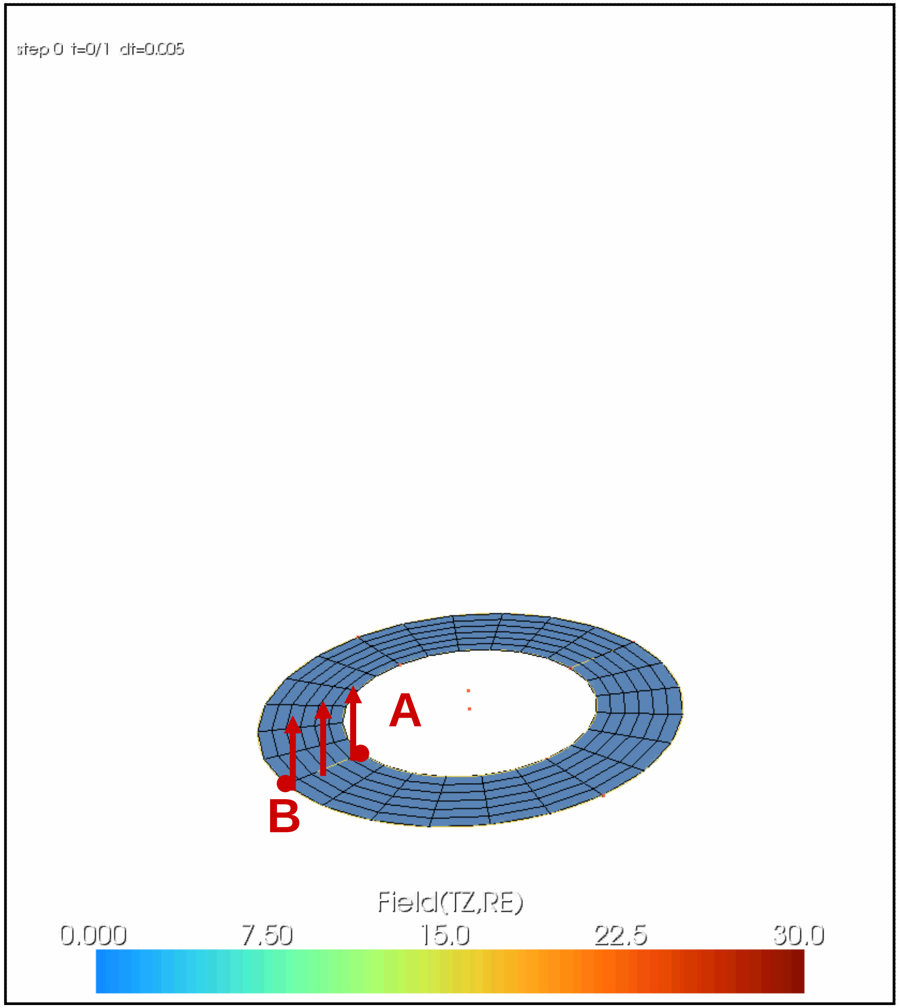

Kirchhoff-Love Shells

- Clamped cylinder
  - Properties:
    - Radius 1.016 m; Length 3.048 m; Thickness 0.03 m
    - Young 20.685 MPa; Poisson 0.3
  - Comparison of DG methods
    - Quadratic & cubic elements
  with literature

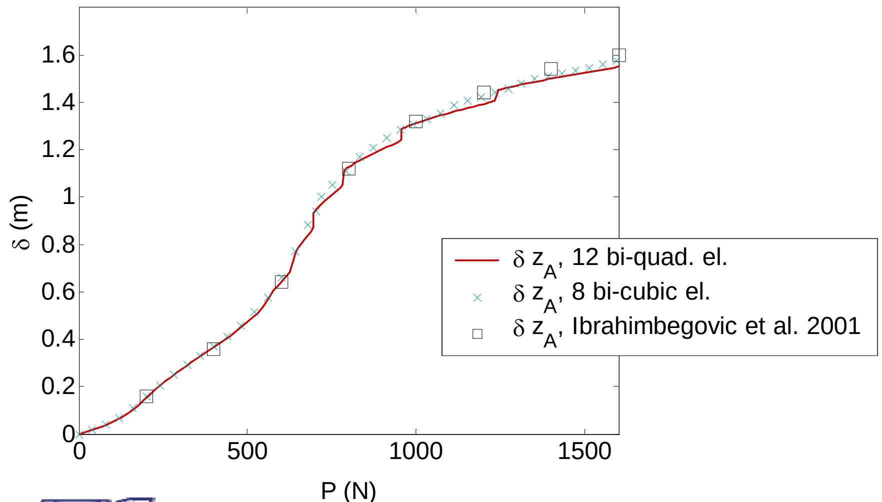

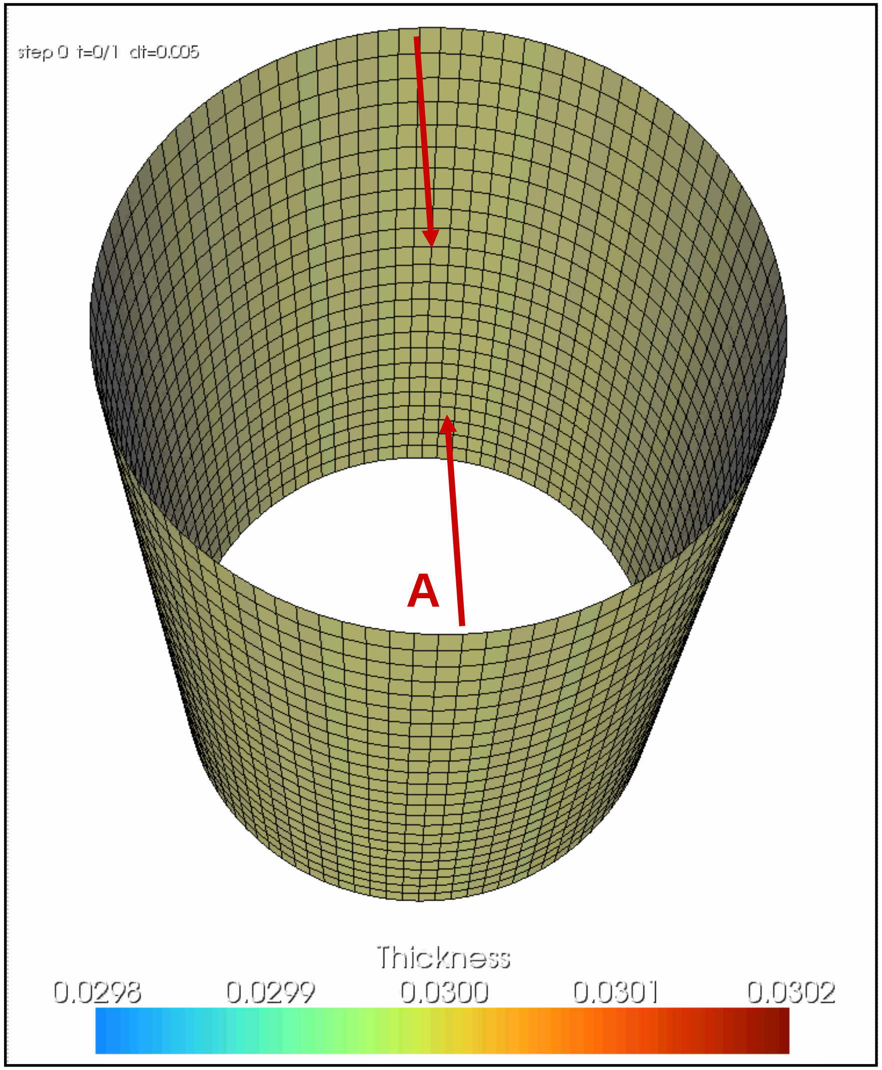

Université de Liège

Dynamic Fracture of thin structures

- Extension of DG/ECL combination to shells
  - We have to substitute the C0/DG formulation by a full DG

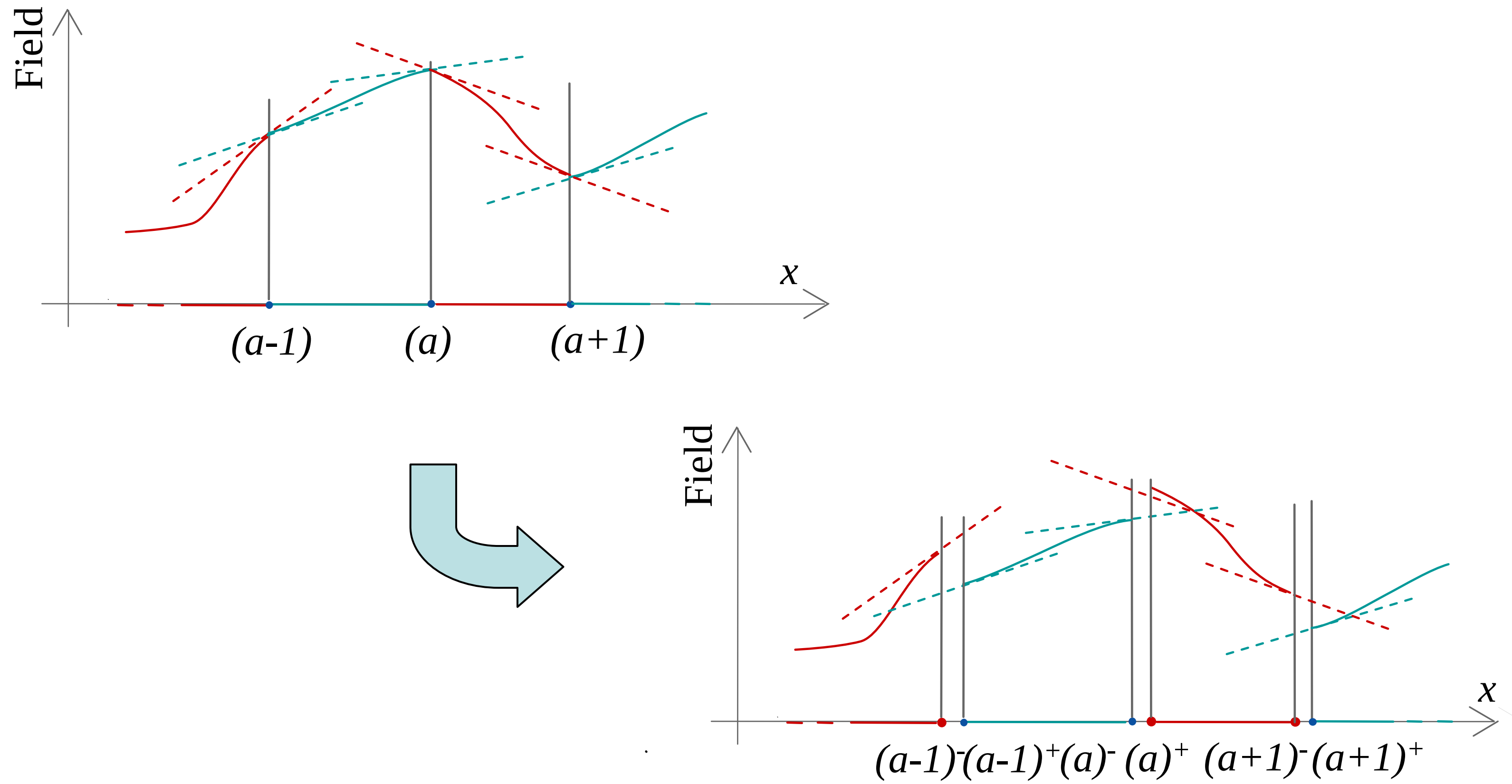

Dynamic Fracture of thin structures

- Kinematics of linear beams
  - Beam's equation are deduced from Kirchhoff-Love shell kinematics
    - So the DG formulations can be related to each other

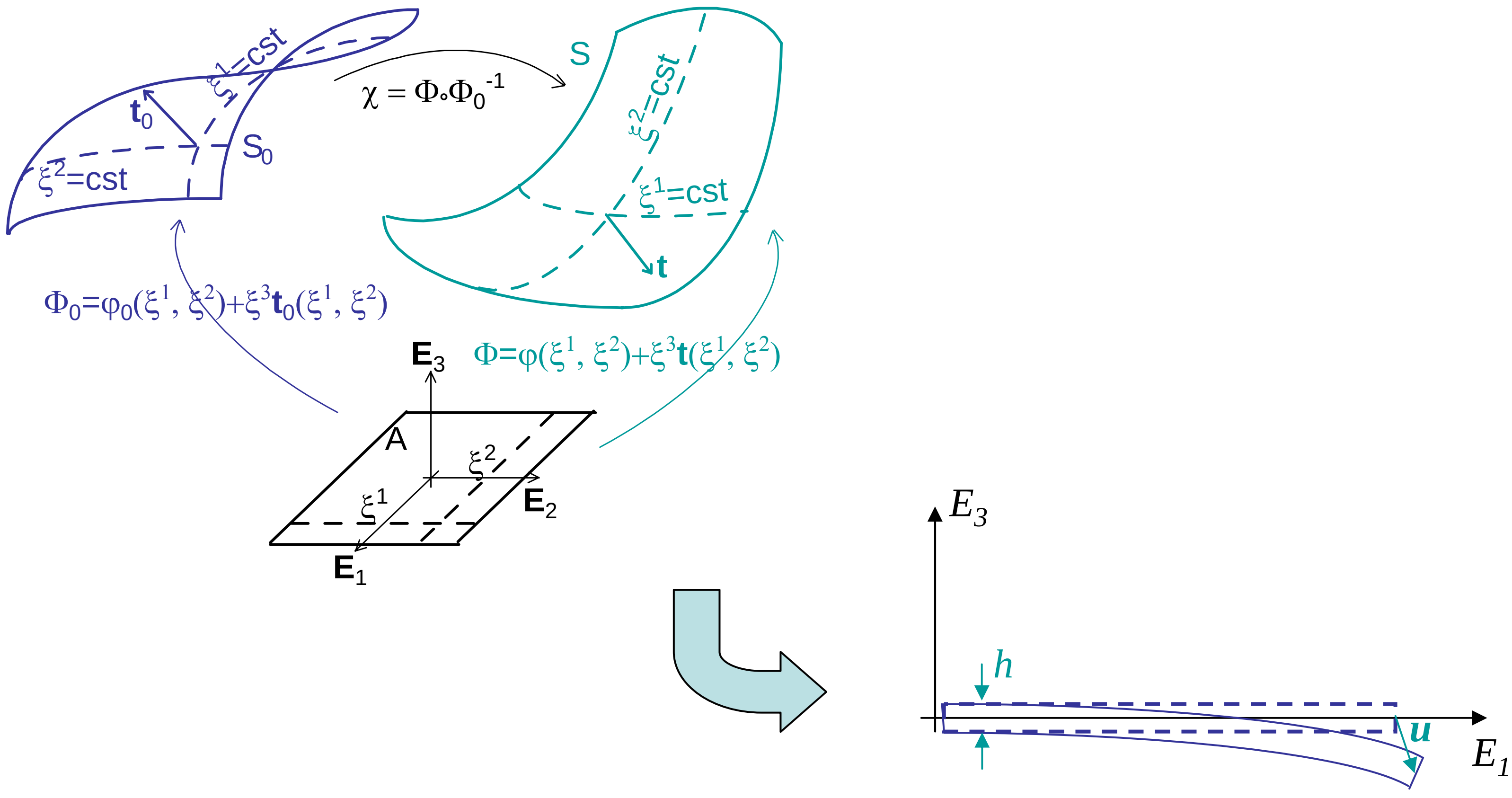

Université de Liège

Dynamic Fracture of thin structures

- Linear momentum equation for linear Euler-Bernoulli beams
  - Resultant stresses
    - $\boldsymbol{n}^{\alpha} = \frac{1}{\bar{j}} \int_{h_{\min 0}}^{h_{\max 0}} \boldsymbol{\sigma} \boldsymbol{g}^{\alpha} \det(\boldsymbol{\nabla \Phi}) \, d\xi^3$ & $\boldsymbol{l} = \frac{1}{\bar{j}} \int_{h_{\min 0}}^{h_{\max 0}} \boldsymbol{\sigma} \boldsymbol{g}^{3} \det(\boldsymbol{\nabla \Phi}) \, d\xi^3$
    - Only the component along x-axis is non-zero

$$n^{11} = \int_{h_{min}}^{h_{max}} \sigma_{11} d\xi^3 = \int_{h_{min}}^{h_{max}} \left(E(u_{1,1} - u_{3,11}\xi^3) \right) d\xi^3 = Ehu_{1,1}$$

  - Resultant equation (no volume forces)

$$\frac{1}{\bar{j}} \left(\bar{j} \boldsymbol{n}^{\alpha} \right)_{,\alpha} + \boldsymbol{n}^{A} = 0 \quad \Rightarrow \quad n^{11}_{,1} = 0$$

Dynamic Fracture of thin structures

- Angular momentum equation for linear Euler-Bernoulli beams
  - Resultant bending stresses
    - $\tilde{\boldsymbol{m}}^{\alpha} = \frac{1}{\bar{j}} \int_{h_{\min 0}}^{h_{\max 0}} \xi^3 \boldsymbol{\sigma} \boldsymbol{g}^{\alpha} \det(\boldsymbol{\nabla \Phi})\, d\xi^3$ & $\boldsymbol{l} = \frac{1}{\bar{j}} \int_{h_{\min 0}}^{h_{\max 0}} \boldsymbol{\sigma} \boldsymbol{g}^{3} \det(\boldsymbol{\nabla \Phi})\, d\xi^3$
    - Only the component along *x*-axis is non-zero

$$\tilde{m}^{11} = \int_{h_{min}}^{h_{max}} \sigma_{11} \xi^3 d\xi^3 = \int_{h_{min}}^{h_{max}} \left(E(u_{1,1} - u_{3,11}\xi^3) \right) \xi^3 d\xi^3 = -\frac{Eh^3}{12} u_{3,11}$$

    - In order to develop a full dg formulation we keep the shearing term $\boldsymbol{l}_1$

$$n^{31} = \int_{h_{min}}^{h_{max}} \sigma_{31} d\xi^3 = \int_{h_{min}}^{h_{max}} \left(\frac{E}{2(1+\nu)} (u_{3,1} + \overline{\theta}) \right) d\xi^3 = \frac{Eh}{2(1+\nu)} (u_{3,1} + \overline{\theta})$$

  - Resultant equation (no volume forces)

$$\frac{1}{\bar{j}} \left(\bar{j} \tilde{\boldsymbol{m}}^{\alpha} \right)_{,\alpha} - \boldsymbol{l} + \lambda \boldsymbol{t} + \tilde{\boldsymbol{m}}^{\mathcal{A}} = 0 \quad \Longrightarrow \quad \tilde{m}^{11}_{,1} - n^{31} = 0$$

Dynamic Fracture of thin structures

- Full DG formulation of linear Euler-Bernoulli beams
  - From the 2 equations
    - $n^{11}_{,1} = 0$ & $\tilde{m}^{11}_{,1} - n^{31} = 0$
  - The weak formulation reads
    - $\int_0^L \left[n^{11}_{,1}\delta u_1 + \tilde{m}^{11}_{,1}\delta(-u_{3,1}) - n^{31}\delta(-u_{3,1})\right] dx = 0$

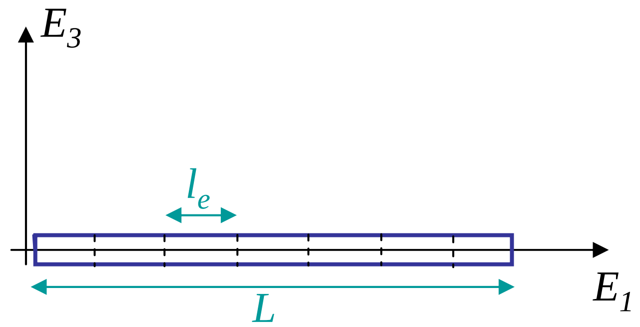

    - As shape functions and their derivatives are discontinuous, the integration by parts becomes

$$\sum_e \left\{ \int_{l_e} \left[n^{11}\delta u_{1,1} + \tilde{m}^{11}\delta(-u_{3,11}) - n^{31}_{,1}\delta(-u_3)\right] dx - \left(\left[n^{11}\delta u_1\right]_{l_e} + \left[\tilde{m}^{11}\delta(-u_{3,1})\right]_{l_e} - \left[n^{31}\delta(-u_3)\right]_{l_e} \right) \right\} = 0$$

    - 3 interface terms that will be treated as before, each one will give
      - A consistency term
      - A symmetric term
      - A stabilization term

Except the shearing term, as $n^{31} = 0$ (applies to the consistency and symmetric terms)

Dynamic Fracture of thin structures

- Full DG formulation of linear Euler-Bernoulli beams (2)
  - The weak formulation reads (2)
    - From

$$\sum_e \left\{ \int_{l_e} \left[n^{11}\delta u_{1,1} + \tilde{m}^{11}\delta(-u_{3,11}) - n^{31}_{,1}\delta(-u_3)\right] dx - \left(\left[n^{11}\delta u_1\right]_{l_e} + \left[\tilde{m}^{11}\delta(-u_{3,1})\right]_{l_e} - \left[n^{31}\delta(-u_3)\right]_{l_e} \right) \right\} = 0$$

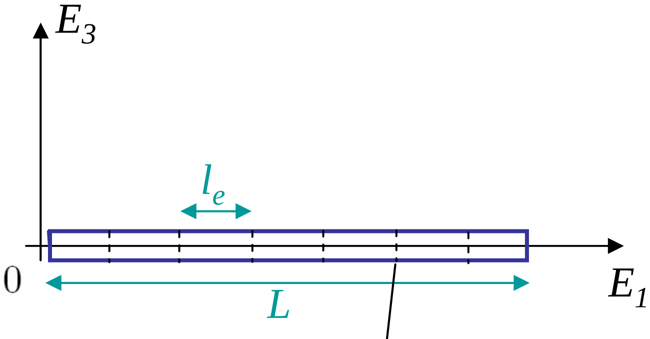

$$a(\boldsymbol{u}, \delta\boldsymbol{u}) = \sum_e \int_{l_e} \left[n^{11}\delta u_{1,1} + \tilde{m}^{11}\delta(-u_{3,11})\right] dx +$$

$$\sum_s \Bigg(\langle n^{11}\rangle [\![\delta u_1]\!] + \langle Eh\delta u_{1,1}\rangle [\![u_1]\!] + [\![u_1]\!] \left\langle \frac{\beta_2 Eh}{h_s} \right\rangle [\![\delta u_1]\!] +$$

$$\langle \tilde{m}^{11}\rangle [\![\delta(-u_{3,1})]\!] + \left\langle \frac{Eh^3}{12}\delta(-u_{3,11}) \right\rangle [\![-u_{3,1}]\!] + [\![-u_{3,1}]\!] \left\langle \frac{\beta_1 Eh^3}{12 h_s} \right\rangle [\![-\delta u_{3,1}]\!] +$$

$$[\![u_3]\!] \left\langle \frac{\beta_3 Eh}{2(1+\nu)h_s} \right\rangle [\![\delta u_3]\!] \Bigg) = 0$$

- As before, DG terms are integrated using interface elements

Université de Liège

Dynamic Fracture of thin structures

- Full DG/ECL combination for Euler-Bernoulli beams
  - When rupture criterion is satisfied at an interface element
    - Shift from
      - DG terms ($\alpha_s = 0$) to
      - Cohesive terms ($\alpha_s = 1$)

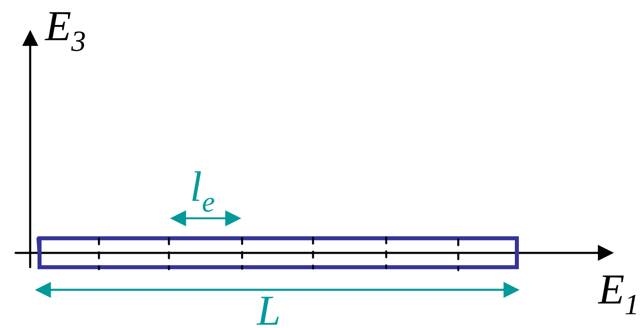

$$\sum_n \int_{l_e} \left[n^{11}\delta u_{1,1} + m^{11}\delta(-u_{3,11})\right] dx +$$

$$\sum_s (1-\alpha_s)\Big(\langle n^{11}\rangle [\![\delta u_1]\!] + \langle Eh\delta u_{1,1}\rangle [\![u_1]\!] + [\![u_1]\!] \left\langle \frac{\beta_2 Eh}{h_s}\right\rangle [\![\delta u_1]\!] + \langle m^{11}\rangle [\![\delta(-u_{3,1})]\!] + \left\langle \frac{Eh^3}{12}\delta(-u_{3,11})\right\rangle [\![-u_{3,1}]\!] + [\![-u_{3,1}]\!]\left\langle\frac{\beta_1 Eh^3}{12h_s}\right\rangle [\![-\delta u_{3,1}]\!]\Big) +$$

$$\sum_s \alpha_s \left(N(\Delta^*)\delta[\![u_1]\!] + M(\Delta^*)\delta[\![-u_{3,1}]\!]\right) + \sum_s [\![\delta u_3]\!]\left\langle \frac{\beta_3 Eh}{2(1+\nu)h_s}\right\rangle [\![\delta u_3]\!] = 0$$

  - What remain to be defined are the cohesive terms

Dynamic Fracture of thin structures

- New cohesive law for Euler-Bernoulli beams
  - Should take into account a through the thickness fracture
    - Problem : no element on the thickness
    - Very difficult to separate fractured and not fractured parts
  - Solution:
    - Application of cohesive law on
      - Resultant stress

        $n^{11} \Rightarrow N(\Delta^*)$
      - Resultant bending stress

        $\tilde{m}^{11} \Rightarrow M(\Delta^*)$
    - In terms of a resultant opening Δ^*

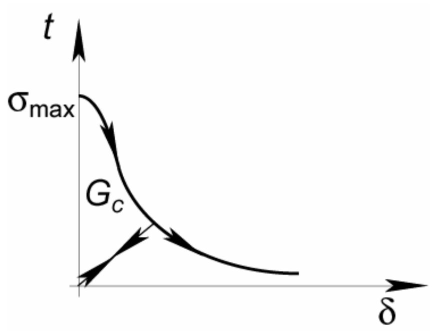

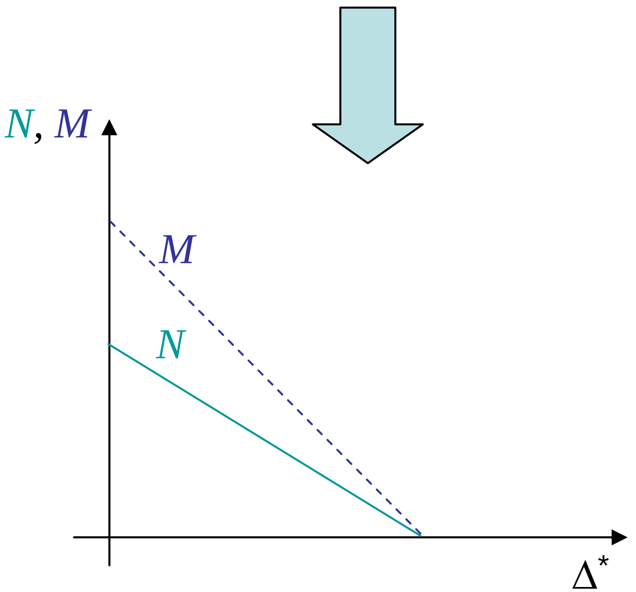

Université de Liège

Dynamic Fracture of thin structures

- Resultant opening Δ^* and cohesive laws $N(\Delta^*)$ & $M(\Delta^*)$
  - Defined such that
    - At fracture initiation
      - $N_0 = N(0)$ and $N_0 = M(0)$ satisfy $\sigma(\pm h/2) = \pm\, \sigma_{max}$
    - After fracture
      - Energy dissipated = $h\, G_C$
  - Solution
    - $\Delta^* = (1-\beta)\Delta_x + \beta \frac{h}{6}\Delta_r$
      - Δ_x: Opening is tension
      - Δ_r: Opening in rotation
      - Coupling parameter

$$\beta = \frac{|6/hM_0|}{N_0 + |6/hM_0|}$$

    - Null resistance for $\Delta^* = \Delta_c = 2G_C/\sigma_{max}$

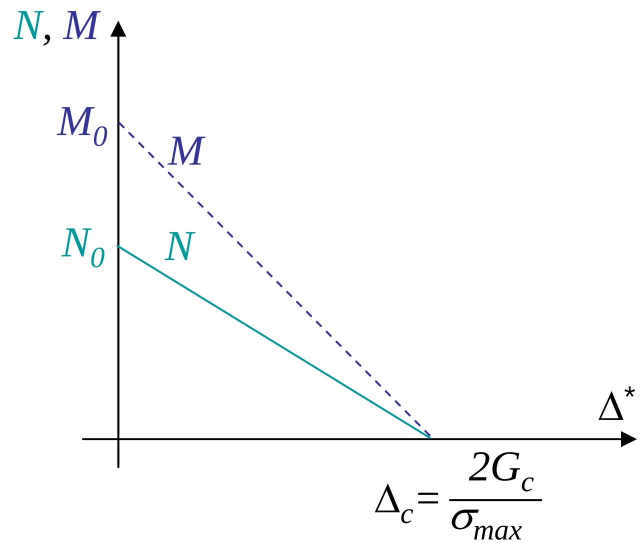

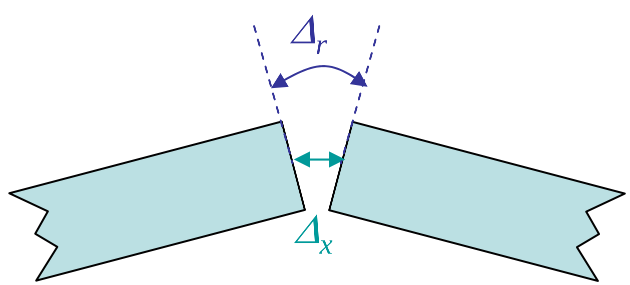

Dynamic Fracture of thin structures

- Numerical example
  - DCB with pre-strain
    - When flexion increases

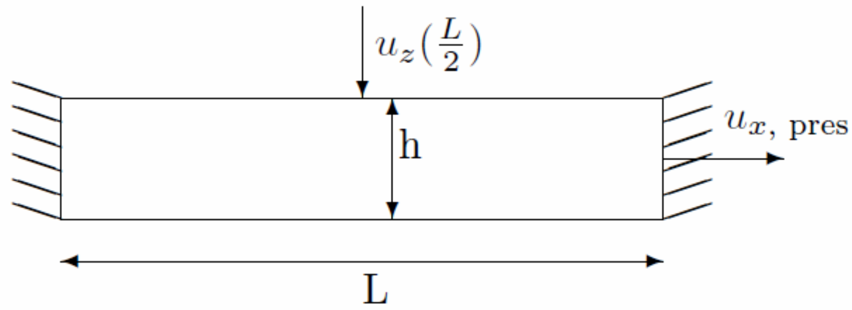

      - When the maximum stress is reached
        - » Beam should shift from a DCB configuration to 2 SCB configurations
    - During the rupture process
      - Either the variation of internal energy is larger than hG_C and rupture should be instable
      - Or the variation of internal energy is smaller than hG_C and rupture should be stable
        - » Complete rupture is achieved only if flexion is still increased
        - » Whatever the pre-strain, after rupture, the energy variation should correspond to hG_C

Dynamic Fracture of thin structures

- Instable fracture
  - Geometry such that variation of internal energy > hG_C

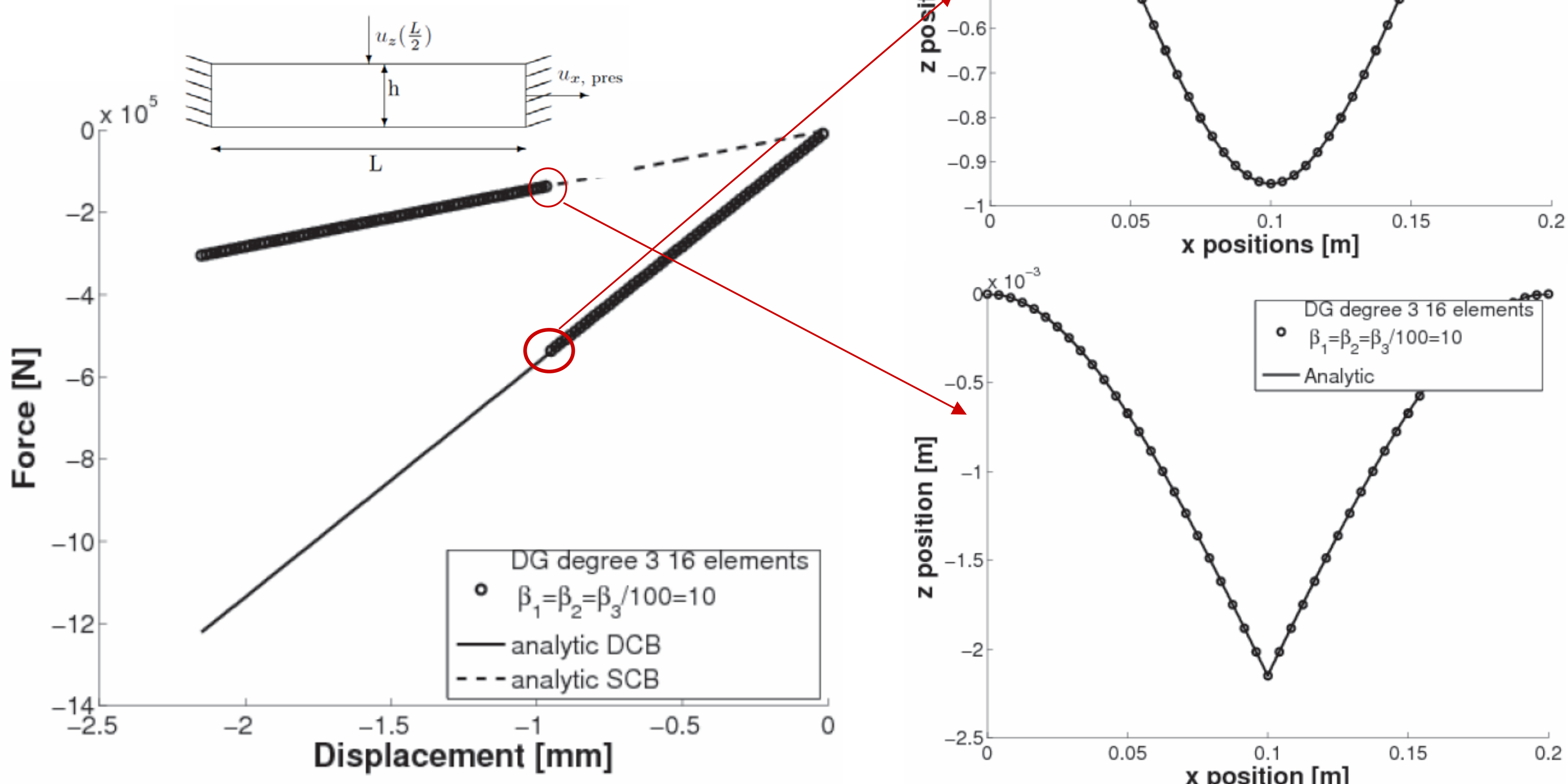

Dynamic Fracture of thin structures

- Stable fracture
  - Geometry such that variation of internal energy < hG_C

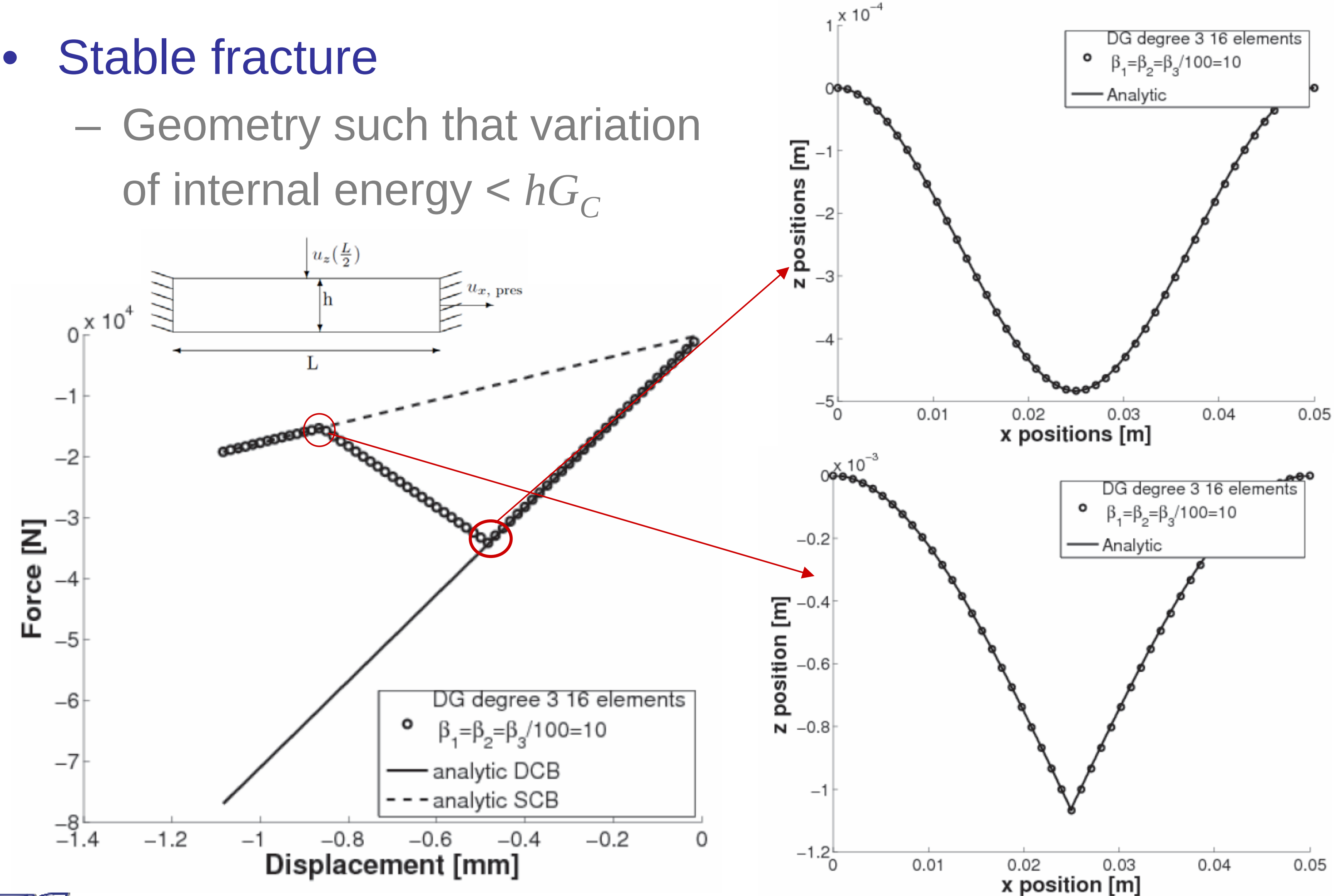

Université de Liège

Dynamic Fracture of thin structures

- Stable fracture
  - Effect of pre-strain
    - Dissipated energy always = hG_C

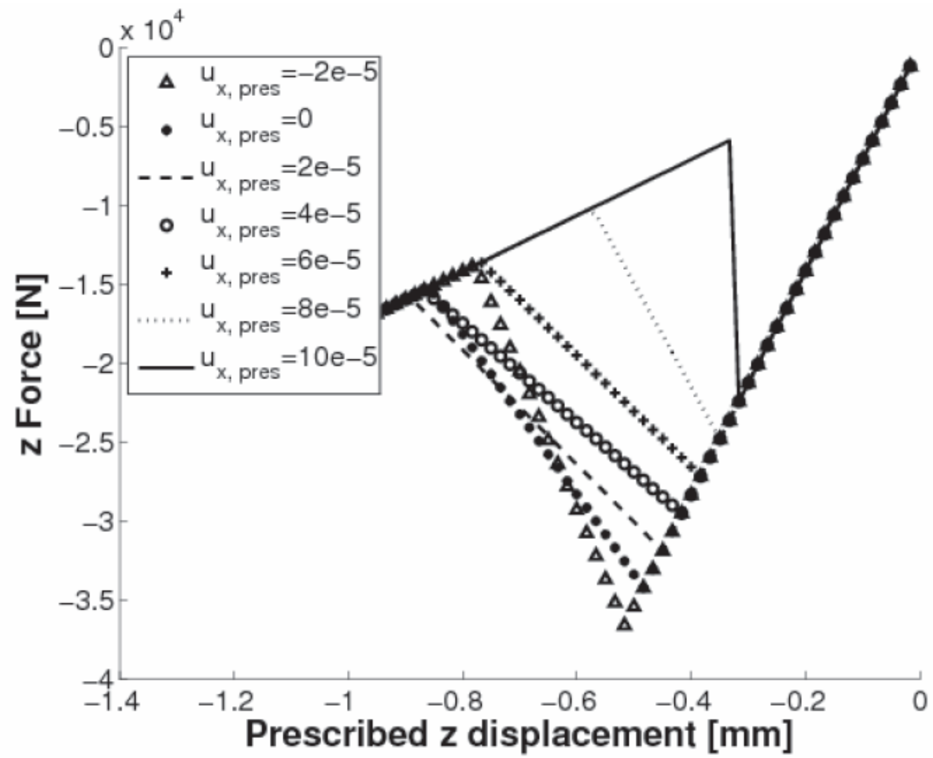

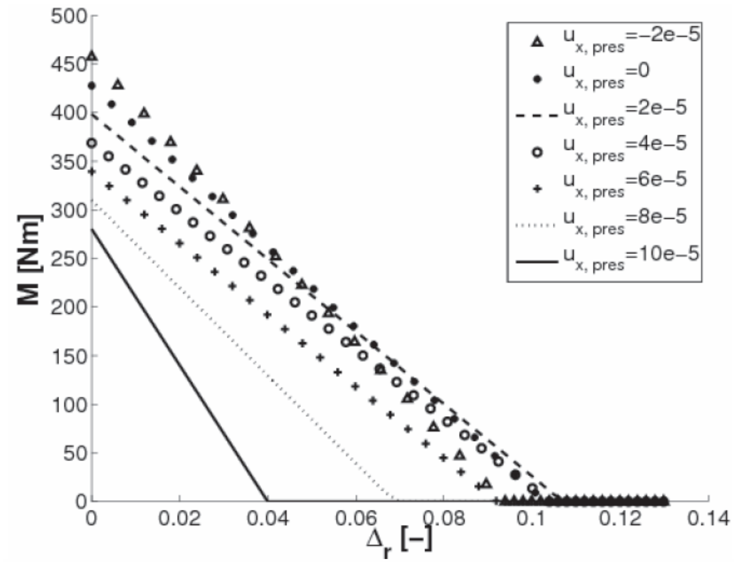

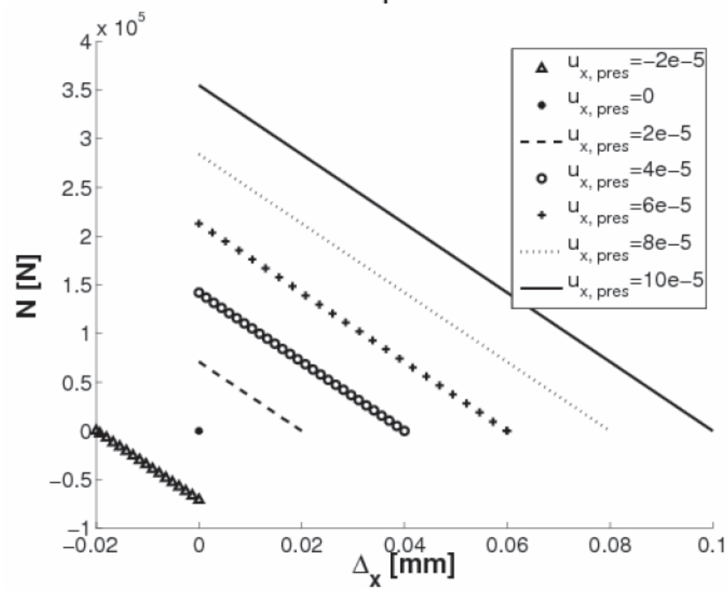

Conclusions & Perspectives

- Development of discontinuous Galerkin formulations
  - Formulation of non-linear dynamics
    - As interface elements exist: cohesive law can be inserted
  - Formulation of high-order differential equations
    - C0/DG formulation of non-linear shells
      - No new degree of freedom
      - No rotation degree or freedom
    - Full DG formulation of beams
      - New degree of freedom
      - No rotation degree or freedom
      - As interface elements exist: cohesive law can be inserted